

Original Article

Abnormality of intestinal cholesterol absorption in *Apc^{Min/+}* mice with colon cancer cachexia

Biao Yu*, Xiao-Huan Peng*, Ling-Yu Wang, An-Bei Wang, Yan-Yan Su, Jia-Huan Chen, Xin-Wei Zhang, Da-Zhong Zhao, He Wang, Da-Xin Pang, Hong-Sheng Ouyang, Xiao-Chun Tang, Ming-Jun Zhang

Jilin Provincial Key Laboratory of Animal Embryo Engineering, College of Animal Sciences, Jilin University, Changchun, Jilin Province, China. *Equal contributors.

Received December 30, 2018; Accepted January 24, 2019; Epub March 1, 2019; Published March 15, 2019

Abstract: Colorectal cancer syndrome has been one of the greatest concerns in the world, particularly in developed countries. Several epidemiological studies have shown that dyslipidemia may be associated with the progression of intestinal cachexia, but there is little research on the function of the small intestine, which is involved in blood lipid metabolism, in dyslipidemia. In the present study, we aimed to explore the function of intestinal cholesterol absorption in the *Apc^{Min/+}* mouse model using an intestinal lipid absorption test. We found that both triglyceride (TG) and total cholesterol (TC) uptake were inhibited in the intestine of *Apc^{Min/+}* mice with age and the intestinal peroxisome proliferator-activated receptor α (PPAR α) downregulated the processes of β -oxidation, oxidative stress response, and cholesterol absorption in APC-deficient mice. In addition, reduced expression levels of farnesoid X receptor (FXR) and apical sodium-dependent bile acid transporter (ASBT) indicated that bile acid metabolism might be associated with intestinal cholesterol absorption in *Apc^{Min/+}* mice. Thus, our data suggested that the intestine plays an essential role in cholesterol uptake and that bile acid metabolism seems to cause a decrease in intestinal cholesterol uptake in *Apc^{Min/+}* mice.

Keywords: Adenomatous polyposis coli (APC), cholesterol absorption, dyslipidemia, peroxisome proliferator-activated receptor α (PPAR α), bile acid

Introduction

Colorectal cancer (CRC) syndrome has been one of the greatest concerns in the world, particularly in developed countries [1]. A classic animal model of human familial adenomatous polyposis (FAP) is the C57BL/6J-*Apc^{Min/+}* mouse, and this mouse has a truncated mutation in the adenomatous polyposis coli (APC) gene, which results in multiple intestinal adenoma polyps and is associated with the loss of muscle and fat accompanying hyperlipidemia [2, 3]. Hyperlipidemia has been reported to be closely associated with the development of intestinal adenoma polyps in the *Apc^{Min/+}* mouse [4]. Previous studies have shown that a low level of intestinal lipoprotein lipase (LPL) mRNA expression may be involved in dyslipidemia and tumor progression [2]. However, what we often ignore is the role of the small intestine in the process of blood lipid metabolism.

Epithelial cells are an important part of the lipid balance in the intestine. Not only can epithelial cells of the small intestine absorb approximately 95% triglycerides (TGs), but they can also store TGs within cytosolic lipid droplets (CLDs) [5, 6]. In addition, the absorbed TGs are decomposed in the lumen of the gut, resulting in FFAs that are activated, esterified and released into lymphatic circulation [7, 8]. CLDs play a core role in the control of enterocyte triglyceride-rich lipoprotein (TRL) secretion [9].

Previous studies have shown that peroxisome proliferator-activated receptor α (PPAR α) can regulate the serum level of TGs in *Apc^{Min/+}* mice through administering the PPAR α ligand bezafibrate [2]. Interestingly, recent studies have emphasized the importance of PPAR α in regulating several important processes such as β -oxidation, the oxidative stress response and cholesterol absorption in the murine small

Intestinal cholesterol absorption in colorectal cancer

Table 1. Primer pairs used for the qRT-PCR analysis

Target gene	Primer sequence (5'-3')	Reverse primer sequence (5'-3')
AOX	CCTGTTGGCCTCAATTA	GGTCATATGTGGCAGTGGTT
ACOT1	GGAGTTGGAGGTGGCCTTCT	CGCAGGTAGTTCACGGCTTC
ACOT2	GCACGAGCGTCACTTCTTGG	CCGATACTCCAGAAGGCCAC
ACAA2	GGACTTCTCTGCACCGATT	AGAGCCACAGAGCCTGTGA
GSTK1	AAGCAGTCTTCCAGGTTC	CCAGAATGCTCTGATACTCC
GSTM3	ATGCCATCCTGCGCTACCT	CCAGGAAGCTCAGAGTAGAGC
GSST	CTGTACCTGGATCTGCTGTC	TAGCCACACTCTCACACAGG
NPC1L1	TGTCCCGCCTATAACAATGG	CCTTGGTGATAGACAGGCTACTG
CD36	GCAGGTCTATCTACGCTGTG	GGTTGTCTGGATTCTGGAGG
MTTP	GTCAACAGAGAGGCGAGAAG	CTAGCCAAGCCTCTCTTGAG
ABCA1	CTCTTCATGACTCTAGCCTGGA	ACACAGACAGGAAGACGAACAC
ABCG5	AGAGGGCCTCACATCAACAGA	CTGACGCTGTAGGACACATGC
ABCG8	AGTGGTCAGTCCAACACTCTG	GAGACCTCCAGGTATCTTGAA
FXR	GCTTGATGTGCTACAAAAGCTG	CGTGGTGATGGTTGAATGTCC
ASBT	GTACAATGGTGGAGCACAGC	GTGCCTGGATCATTGAACCC
GAPDH	TTGTCTCTGCGACTTCA	CACCACCCTGTTGCTGTA

intestine, which may represent risk factors for hyperlipidemia [10-12]. However, there are few studies on the roles of β -oxidation, the oxidative stress response and cholesterol absorption in hyperlipidemia; therefore, the exact mechanism remains unclear.

Thus, whether PPAR α signaling regulates intestinal cholesterol absorption in *Apc*^{Min/+} mice and the exact mechanism of its action are unclear. Therefore, we explored the intestinal cholesterol absorption ability of *Apc*^{Min/+} mice using an intestinal lipid absorption test. The aim of this study was to reveal the potential reason for lipid absorption abnormalities in the intestine of *Apc*^{Min/+} mice.

Materials and methods

Animals

Four- to five-week-old wild-type male C57BL/6J (WT, n=20) and mutant male C57BL/6J-*Apc*^{Min/+} (*Apc*^{Min/+}, Min, n=20) mice were purchased from the Nanjing Biomedical Research Institute of Nanjing University (Nanjing, China). The mice were provided standard rodent chow and water *ad libitum* and housed in cages (≤ 5 mouse per cage) that were placed in an SPF animal facility with the laboratory temperature maintained at 22°C and 40-60% humidity with a 12:12 light: dark cycle. All animal welfare and experimental procedures were performed strictly according to the National Institutes of Health guide for the

care and use of laboratory animals (NIH Publications No. 8023, revised 1978). In addition, the procedures were approved by the Institutional Animal Care and Use Committee of Jilin University under approved protocol number 201707025.

Intestinal lipid absorption test

At the periods of 8, 14 and 20 weeks, the mice were fasted for 4 hours starting at 05:00 prior to undergoing the intestinal lipid absorption test. Thirty minutes after injection, the mice were gavaged with 200 μ l of olive oil to assess dietary fat

absorption. Blood was sampled via the tail vein at the baseline of 0 h and at 3 and 6 h, and the blood was centrifuged at 2000 \times g for 10 minutes at 4°C. Fasting plasma total cholesterol (TC) and triglycerides (TGs) were analyzed using commercial kits from Biosino (Beijing, China) [13].

Intestinal permeability assay

FITC-dextran (4 kDa, Sigma, USA) was administered by oral gavage (60 mg/100 g body weight, 40 mg/mL) to the fasted mice. After 1 hour, blood was collected, stored on ice in the dark and centrifuged 1000 \times g for 15 minutes at 4°C. The serum was diluted with the same volume of PBS, and the fluorescence intensity was measured using a fluorescence spectrophotometer (λ_{ex} : 485 nm; λ_{em} : 535 nm, Infinite 200 Pro, Tecan, Switzerland) [14].

Gut transit test

Overnight-fasted mice were gavaged with 200 μ l of Evans blue suspension (5% Evans blue and 5% gum arabic in PBS). Afterward, the mice had free access to food and water, and the time until the Evans blue was detected in the feces was recorded [13].

Oil red O staining

For oil red O staining, the jejunum was isolated and fixed in 4% neutral-buffered formalin (Carl

Intestinal cholesterol absorption in colorectal cancer

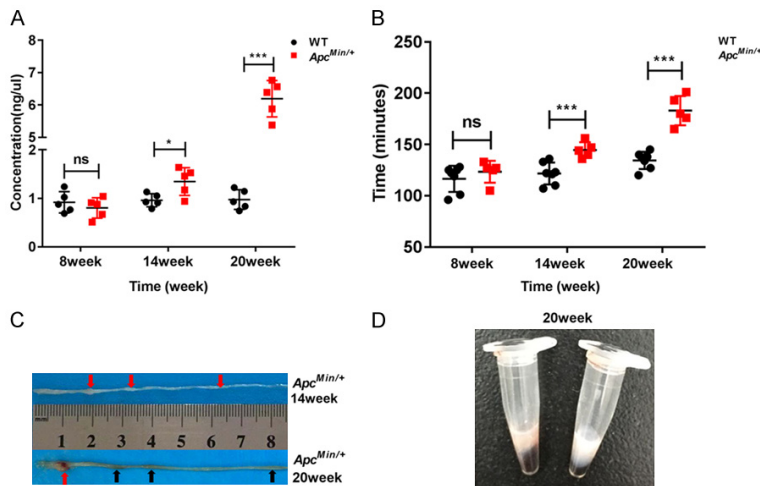


Figure 1. Gut barrier dysfunction in *Apc^{Min/+}* mice with colon cancer cachexia. A. Gut permeability was measured between the *Apc^{Min/+}* mice and the WT mice at 8, 14, and 20 weeks of age. Serum fluorescein dextran concentrations were measured one hour after gavage (n=5). B. Mice were gavaged with 200 μ l of Evans blue, and gut transit was determined by recording the time until Evans blue appeared in the feces (WT=7, *Apc^{Min/+}*=5). C. Cachexia (red arrow) in the intestine at 14 and 20 weeks of age in *Apc^{Min/+}* mice. Intestinal inflammation (black arrow) in the intestine at 20 weeks of age in *Apc^{Min/+}* mice. D. Lactescent serum of the *Apc^{Min/+}* mouse was observed at 20 weeks of age. Data are expressed as the Mean \pm SEM. The differences between the mean values were assessed by Student's t-tests and analyzed using GraphPad Prism software 7.0. * P <0.05; *** P <0.001; ns, not significant.

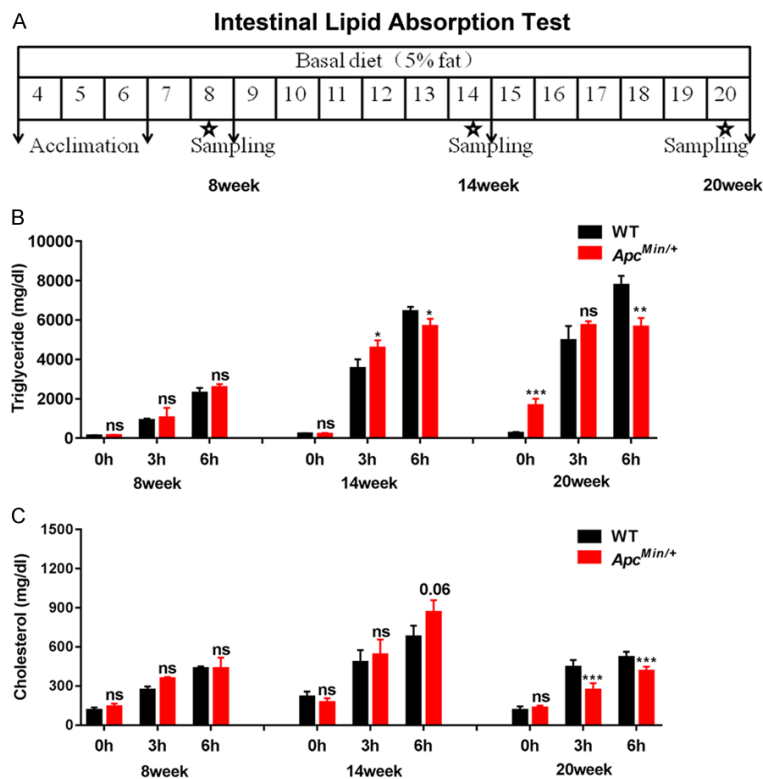


Figure 2. Intestinal lipid absorption inhibition occurs in *Apc^{Min/+}* mice. A. Study schematic of the intestinal lipid absorption test at 8, 14 and 20 weeks of age in mice. B and C. Plasma triglyceride (TG) and total cholesterol (TC) levels were determined by tail vein nick in the *Apc^{Min/+}* and WT mice at 0-, 3- and 6-h time points at 8, 14 and 20 weeks (n \geq 5). Data are the mean of three independent experiments (an average of five readings was conducted for each sample), Mean \pm SEM. The differences between the mean values were assessed by Student's t-tests and analyzed using GraphPad Prism software 7.0. * P <0.05; ** P <0.01; *** P <0.001 and ns, not significant.

Roth GmbH, Vienna, Austria). Serial sections (5 μ m) of the jejunum were removed and stained with oil red O and Mayer's hematoxylin. Microscopic images were taken using a Nikon Eclipse E600 equipped with a Nikon Digital Sight DS-U1 unit (Spach Optics Inc., New York, NY). Oil Red O staining of the jejunum was performed on frozen sections using standard protocols [15].

Real-time quantitative PCR analysis

Total RNA from the jejunum of mice was extracted using TRNzol-A reagent and reverse transcribed to cDNA according to the manufacturer's instructions using a FastQuant RT kit (Tiangen, Beijing, China). The primers used for gene amplification are presented in **Table 1**. qPCR was performed using a Bio-RadiQ5 instrument (Bio-Rad, USA). The $2^{-\Delta\Delta Ct}$ method was used to determine related gene expression, which was normalized to the amount of GAPDH mRNA. All experiments were repeated three times

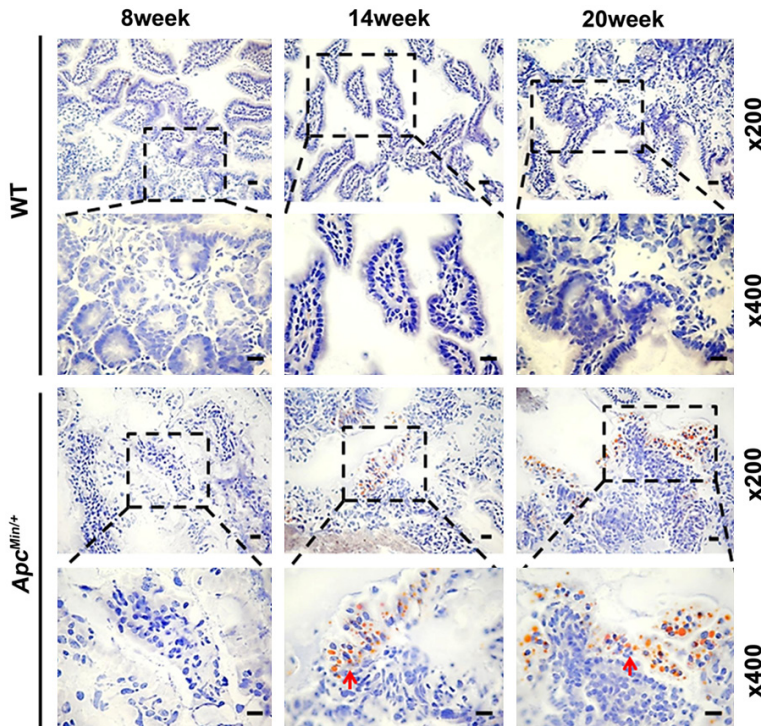


Figure 3. Lipid droplets accumulate in the jejunum of *Apc^{Min/+}* mice. Oil red O staining revealed the accumulation of lipid droplets (red arrow) in the intestine of *Apc^{Min/+}* mice at 14 weeks and 20 weeks of age. Magnification, $\times 200$ and $\times 400$. Scale bars: 50 μm .

for each gene and the data are expressed as the mean \pm SEM.

Western blotting analysis

Equal amounts of protein samples were loaded into each lane of the gel for SDS-PAGE, followed by immunoblotting on a nitrocellulose membrane (NC, Boster, China). Then, the membranes were incubated with an LPL antibody and a PPAR α antibody (Boster, China) at 4°C. The membranes were incubated with a secondary antibody (GAPDH, Beyotime, China) and imaged using a BeyoECL Plus kit (Beyotime, Beijing, China). To confirm the reproducibility of the results, at least three mice per group were used in each stage or treatment in this study.

Statistical analysis

All the data were analyzed using GraphPad Prism software 7.0 (La Jolla, CA, USA). The variation was analyzed by Student's t-tests, and the results are expressed as the Mean \pm SEM. *P* values < 0.05 were considered statistically significant.

Results

The intestines that were examined in our study were taken from *Apc^{Min/+}* mice and classified as noncachectic (8 weeks of age), precachectic (14 weeks of age) and severely cachectic (20 weeks of age).

Gut barrier dysfunction in *Apc^{Min/+}* mice with colon cancer cachexia

To objectively assess intestinal dysfunction in *Apc^{Min/+}* mice, the permeability of FITC-dextran (4 kDa) was investigated. It was remarkable that the concentration of FITC-dextran increased by nearly 1.5-fold at 14 weeks of age (*Apc^{Min/+}* mouse group versus wild-type mouse group: 1.35 ± 0.29 ng/ μL versus 0.96 ± 0.13 ng/ μL , *P* < 0.05) and approximately 6.5-fold at 20 weeks of age (*Apc^{Min/+}* mouse group versus wild-type mouse

group: 6.19 ± 0.56 ng/ μL versus 0.98 ± 0.2 ng/ μL , *P* < 0.001 ; **Figure 1A**). We noted that the time that Evans blue appeared in the feces gradually increased in the gut transit test at 8, 14 and 20 weeks of age (*Apc^{Min/+}* mouse group versus wild-type mouse group: 123.4 ± 10.71 minutes versus 116.57 ± 12.74 minutes, *P* > 0.05 ; 144.6 ± 7.6 minutes versus 121.71 ± 10.7 minutes, *P* < 0.001 ; 183 ± 14.2 minutes versus 134.43 ± 8.42 minutes, *P* < 0.001 ; respectively; **Figure 1B**). During the deterioration of cachexia (red arrow), significant intestinal inflammation (black arrow) appeared at 20 weeks of age but not at 14 weeks of age in the *Apc^{Min/+}* mice (**Figure 1C**). A remarkable lactescence in *Apc^{Min/+}* mice indicated that the mice had suffered from severe hyperlipidemia (**Figure 1D**).

Intestinal lipid absorption inhibition occurs in *Apc^{Min/+}* mice

To evaluate the intestinal lipid absorption ability of *Apc^{Min/+}* mice, in our study, mice were fasted for 4 h prior to undergoing an intestinal lipid absorption test (**Figure 2A**). Next, we examined

Intestinal cholesterol absorption in colorectal cancer

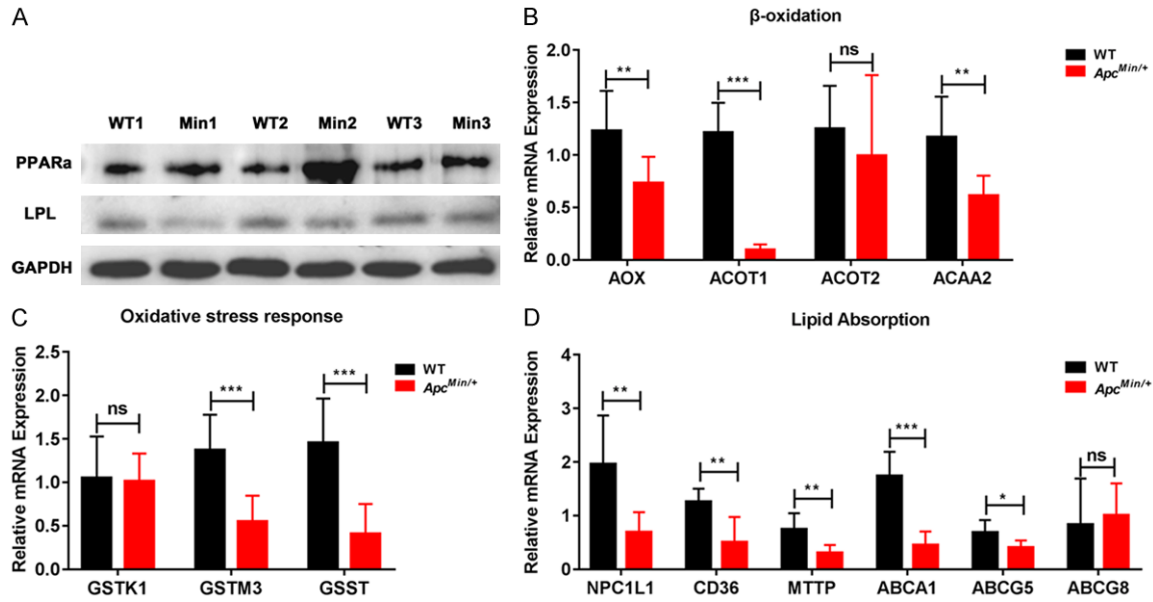


Figure 4. APC deficiency results in the downregulation of intestinal PPAR α target genes. A. LPL and PPAR α proteins were measured by western blot with specific antibodies in the intestine of the *Apc^{Min/+}* and WT mice (WT: wild type mouse, Min: *Apc^{Min/+}* mouse, n=3). B-D. *Aox*, *Acot1*, *Acot2*, *Acaa2*, *Gstk1*, *Gstm3*, *Gsst*, *Npc1l1*, *CD36*, *Mttp*, *Abca1*, *Abcg5* and *Abcg8* were measured by qRT-PCR in the intestine of *Apc^{Min/+}* and the WT mice (n=3). Data are expressed as the Mean \pm SEM. The differences between the mean values were assessed by Student's t-tests and analyzed using GraphPad Prism software 7.0. * $P < 0.05$, ** $P < 0.01$ and *** $P < 0.001$ and ns, not significant.

the levels of serum triglycerides (TGs) and total cholesterol (TC) in *Apc^{Min/+}* and WT mice at 0-, 3-, and 6-hour time points at 8, 14 and 20 weeks after olive oil gavage, respectively. TG was higher in the *Apc^{Min/+}* mice than in the WT mice at the 3-hour time point at 14 weeks (*Apc^{Min/+}* group versus WT group: 4567.55 ± 404.14 mg/dL versus 3541.24 ± 465.15 mg/dL; $P < 0.05$); however, TG was significantly lower in the *Apc^{Min/+}* mice than in the WT mice at the 6-hour time point at 14 weeks (*Apc^{Min/+}* group versus WT group: 5667.14 ± 392.49 mg/dL versus 6305.72 ± 114.7 ; $P < 0.01$). In contrast, TG was significantly higher in the *Apc^{Min/+}* mice than in the WT mice at the 0-hour time point at 20 weeks (*Apc^{Min/+}* group versus WT group: 1659.99 ± 342.28 mg/dL versus 250.02 ± 62.15 mg/dL; $P < 0.001$). However, TG was significantly lower in the *Apc^{Min/+}* group than in the WT group at the 6-hour time point at 20 weeks (*Apc^{Min/+}* group versus WT group: 5647.9 ± 459.72 mg/dL versus 7758.37 ± 488.01 mg/dL; $P < 0.01$). Additionally, there was no significant difference between the WT and *Apc^{Min/+}* mice at 8 weeks, the 0-hour time point at 14 weeks and the 3-hour time point at 20 weeks (**Figure 2B**). The TC of the *Apc^{Min/+}* mice was significantly decreased at the 3-hour and 6-hour

time points at 20 weeks (*Apc^{Min/+}* group versus WT group: 269.7 ± 52.14 mg/dL versus 444.08 ± 54.89 mg/dL; 414.32 ± 33.58 mg/dL versus 519.56 ± 43.71 mg/dL; respectively; $P < 0.001$), and there was no significant difference at 8 and 14 weeks between the two groups (**Figure 2C**).

Lipid droplets accumulate in the jejunum of *Apc^{Min/+}* mice

We further determined whether the intestinal lipid absorption inhibition resulted in lipid droplets accumulating in *Apc^{Min/+}* mice. Oil red O staining of the jejunum confirmed that an increased number of lipid droplets accumulated in the *Apc^{Min/+}* mice than in the WT mice at the 14 and 20 weeks of age and that there was no significant difference at 8 weeks between the two groups (**Figure 3**). Our results indicate that intestinal lipid absorption inhibition occurs in *Apc^{Min/+}* mice with age.

APC deficiency results in the downregulation of intestinal PPAR α target genes

To further understand the function of intestinal lipid metabolism in *Apc^{Min/+}* mice, the expression of PPAR α target genes was analyzed. As is

Intestinal cholesterol absorption in colorectal cancer

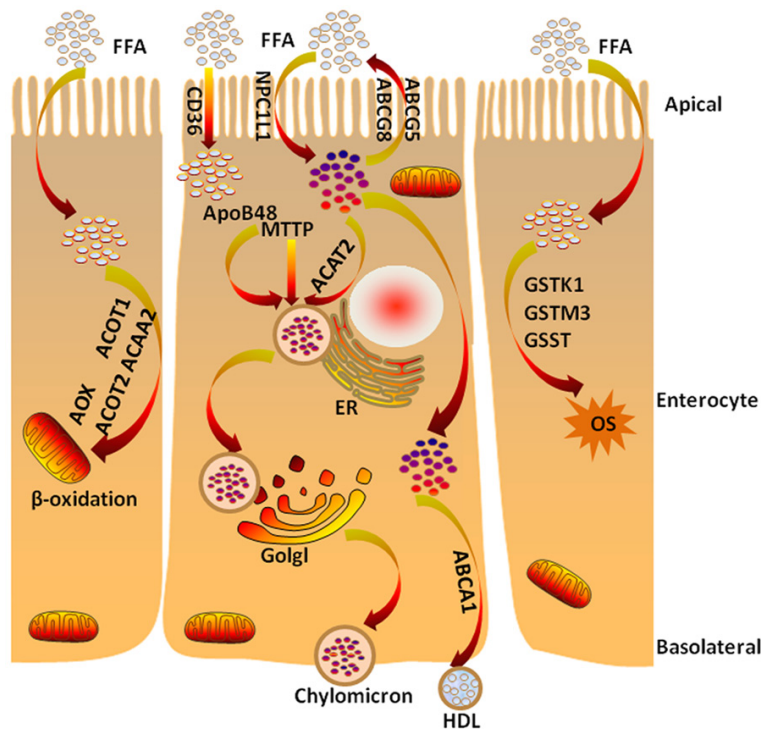


Figure 5. Schematic of fatty acid β -oxidation, oxidative stress response and cholesterol absorption processes in the enterocytes of mouse. The main cholesterol importer NPC1L1 and the cholesterol exporters ABCG5/G8 are located at the apical membrane of enterocytes and facilitate the uptake of cholesterol across the brush border membrane. ACAT2 esterifies the absorbed cholesterol, and MTTP transfers triglycerides and cholesteryl esters to ApoB48 in the smooth ER. The nascent chylomicrons leave the ER, are secreted through the Golgi complex to the basolateral side of the enterocyte and reach the venous circulation through lymphatic vessels. In addition to the chylomicron pathway, a significant portion of intestinal xanthophylls are absorbed through an ABCA1/ApoA1 pathway and may be preferentially delivered to some tissues. The absorption of dietary cholesterol through the apical membrane into enterocytes is associated with β -oxidation and/or oxidative stress response. NPC1L1: Niemann-Pick C1 like-1; ABCG5/G8: ATP-binding cassette transporter G5/G8; CD36: cluster of differentiation 36; apoB48: apolipoprotein B48; MTTP: microsomal triglyceride transfer protein; ACAT2: acyl-coenzyme A cholesterol acyltransferase 2; ER: endoplasmic reticulum; Golgi: Golgi apparatus; ABCA1: ATP-binding cassette transporter A1; HDL: high-density lipoprotein; AOX: acyl-CoA oxidase; ACOT1/2: acyl-CoA thioesterase 1/2; ACAA2: acetyl-CoA acyltransferase 2; GSTK1: glutathione S-transferase kappa 1; GSTM3: glutathione S-transferase mu 3; GSST: glutathione S-transferase theta; OS: oxidative stress; PPAR α : peroxisome proliferator-activated receptor α ; FXR: farnesoid X receptor; ASBT: apical sodium-dependent bile acid transporter; SHP: short heterodimer partner.

reported, a low level of LPL mRNA expression may be associated with dyslipidemia and involved in PPAR α signaling in the intestine of *Apc^{Min/+}* mice [2]. We repeated the experiment and used a western blot analysis in the jejunum of the *Apc^{Min/+}* mice (Figure 4A). Moreover, we determined the expression of intestinal PPAR α target genes: β -oxidation, including acyl-CoA

oxidase (AOX), acyl-CoA thioesterase 1 (ACOT1), acyl-CoA thioesterase 2 (ACOT2) and acetyl-CoA acyltransferase 2 (ACAA2); oxidative stress response (ROS), including glutathione S-transferase kappa 1 (GSTK1), glutathione S-transferase mu 3 (GSTM3) and glutathione S-transferase theta (GSST); lipid absorption, including Niemann-Pick C1 like-1 (NPC1L1), cluster of differentiation 36 (CD36), microsomal triglyceride transfer protein (MTTP), ATP-binding cassette subfamily A member 1 (ABCA1), ATP-binding cassette subfamily G member 5 (ABCG5) and ATP-binding cassette subfamily G member 8 (ABCG8). The expression of *Aox*, *Acot1*, *Acaa2*, *Gstm3*, *Gsst*, *Npc1l1*, *CD36*, *Mttp*, *Abca1* and *Abcg5* was markedly downregulated in the jejunum of the *Apc^{Min/+}* mice. There was no change in the expression of *Acot2*, *Gstk1* and *Abcg8* between the two groups (Figure 4B-D). The results indicated that APC is very important for PPAR α activation in the jejunum. A schematic diagram of the fatty acid β -oxidation, oxidative stress response, and cholesterol absorption processes in the enterocytes of mice is shown in Figure 5.

*Bile acids affect intestinal cholesterol absorption in *Apc^{Min/+}* mice*

CD36 plays an essential role in the uptake of FFAs and cholesterol from the intestinal lumen and is regulated by PPAR α [16, 17]. In our study, decreased CD36, NPC1L1, ABCG5 and ABCA1 mRNA levels might have been involved in the cholesterol absorption inhibition in *Apc^{Min/+}* mice. To further determine whether bile acids can regulate cholesterol absorption, we ana-

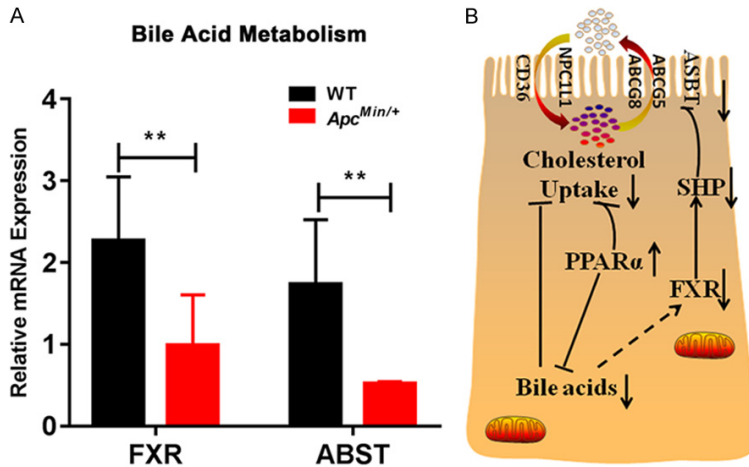


Figure 6. Bile acids affected intestinal cholesterol absorption in *Apc^{Min/+}* mice. **A.** *FXR* and *ASBT* were measured by qRT-PCR in the intestines of *Apc^{Min/+}* and WT mice ($n=3$). Data are expressed as the mean \pm SEM. The differences between the mean values were assessed by Student's t-tests and analyzed using GraphPad Prism software 7.0. $**P<0.01$. **B.** Bile acids may inhibit cholesterol uptake in the intestine of *Apc^{Min/+}* mice. Cholesterol uptake is mediated by NPC1L1, CD36, and ABCG5/G8 in enterocytes. PPAR α activation reduces cholesterol uptake and bile acids and may reduce FXR activation. FXR inhibits ASBT through reduced SHP activation. NPC1L1: Niemann-Pick C1 Like-1; ABCG5/G8: ATP-binding cassette transporter G5/G8; CD36: cluster of differentiation 36; PPAR α : peroxisome proliferator-activated receptor α ; FXR: farnesoid X receptor; ASBT: apical sodium-dependent bile acid transporter; SHP: short heterodimer partner.

lyzed the farnesoid X receptor (FXR) and apical sodium-dependent bile acid transporter (ASBT) mRNA levels between the two groups. The expression of FXR and ASBT was significantly downregulated in the jejunum of the *Apc^{Min/+}* mice ($P<0.01$) (Figure 6A). A schematic of bile acid metabolism in the enterocytes of mice is shown in Figure 6B. These data indicated that intestinal APC deficiency can regulate bile acid metabolism.

Discussion

In our preliminary experiment, we demonstrated that *Apc^{Min/+}* mice exhibit intestinal cachexia that is associated with the loss of body weight and is accompanied by abnormalities in hepatic lipid metabolism. The intestine is an essential element in the biosynthesis of triglycerides and systemic metabolism [18]. However, research on the intestinal lipid mechanism is still lacking in *Apc^{Min/+}* mice.

Our study showed gut barrier dysfunction with hyperlipidemia and tumor growth was present during cachexia. This dysfunction resulted in a significant increase in the permeability of FITC-

dextran (4 kDa) in the intestine along with a delay in gut transit with age. Similarly, research by Puppa et al. suggested that glucose tolerance, plasma IL-6, TGs, and body temperature are characteristic of endotoxemia, which is accompanied with a change in gut permeability in *Apc^{Min/+}* mice [19]. Another study revealed that some inflammation occurring in intestinal epithelial cells can decrease gut homeostasis [20]. In fact, intestinal lipid absorption plays an essential role in gut lipid homeostasis. Our findings demonstrated that the lipid absorption ability dramatically decreased with age, as shown by marked lipid droplet accumulation in the jejunum of the *Apc^{Min/+}* mice.

Current research has shown that intestinal lipid metabolism plays a key role in the

health of animals and that changes in lipid absorption may induce related diseases [21]. As is reported, PPAR α has an essential role in the progression of intestinal diseases [22]. Thus, we also analyzed the expression of PPAR α and related target genes (including genes involved in β -oxidation, the oxidative stress response and cholesterol absorption) in the jejunum. Our results showed that the expression of *Aox*, *Acot1*, *Acaa2*, *Gstm3*, *Gsst*, *Npc1l1*, *Mttp*, *Abca1* and *Abcg5* was remarkably downregulated in the jejunum of the *Apc^{Min/+}* mice. Specifically, during the process of cholesterol absorption, the most obvious change was a significant decrease in CD36, which, as reported, is important in the uptake of free fatty acids (FFAs) and chylomicron formation and secretion from the proximal intestine [23, 24]. In addition, the mRNA levels of the main cholesterol importer NPC1L1 and the cholesterol exporter ABCG5 decreased [25]. Interestingly, the mRNA expression of ABCA1, which is regulated by PPAR α and associated with cholesterol absorption and high-density lipoprotein (HDL) production, was downregulated [26]. Therefore, all the results indicated that reduced levels of

CD36, NPC1L1, ABCG5 and ABCA1 mRNA might be involved in cholesterol absorption in the jejunum of *Apc^{Min/+}* mouse.

Studies have shown that bile acids, as ligands for the bile acid receptor farnesoid X receptor (FXR), alter the transcription of several genes that are involved in triglyceride synthesis and lipid metabolism [27]. Early clinical studies have found that PPAR α regulates bile acid synthesis, bile acid transport and cholesterol metabolism pathways [28]. In addition, PPAR α has been confirmed to be activated in the intestine of *Apc^{Min/+}* mice. Furthermore, our results indicated that decreased expression of FXR and ASBT in the jejunum modulates bile acid metabolism in *Apc^{Min/+}* mice. Thus, we speculate that the change in cholesterol absorption might be a consequence of a reduced amount of bile acids in the jejunum of *Apc^{Min/+}* mice.

In conclusion, our data suggested that the intestine plays an essential role in cholesterol uptake and that bile acid metabolism seems to cause a decrease in intestinal cholesterol uptake in *Apc^{Min/+}* mice.

Acknowledgements

This work was financially supported by the National Natural Science Foundation of China (Grant No. 31472053 and 31572345), Graduate Innovation Fund of Jilin University (Grant No. 2017094), Program for JLU Science and Technology Innovative Research Team (JL-USTIRT, No. 2017TD-28), and Fundamental Research Funds for the Central Universities.

Disclosure of conflict of interest

None.

Address correspondence to: Ming-Jun Zhang, Jilin Provincial Key Laboratory of Animal Embryo Engineering, College of Animal Sciences, Jilin University, 5333 Xi'an Road, Lvyuan District, Changchun 130062, Jilin Province, China. Tel: (86) 431-87836122; Fax: (86) 431-86758018; E-mail: mjzhang@jlu.edu.cn

References

[1] Takahashi H, Hosono K, Endo H, Nakajima A. Colon epithelial proliferation and carcinogenesis in diet-induced obesity. *J Gastroenterol Hepatol* 2013; 28 Suppl 4: 41-7.

[2] Niho N, Takahashi M, Kitamura T, Shoji Y, Itoh M, Noda T, Sugimura T, Wakabayashi K. Concomitant suppression of hyperlipidemia and intestinal polyp formation in *apc*-deficient mice by peroxisome proliferator-activated receptor ligands. *Cancer Res* 2003; 63: 6090-6095.

[3] Niho N, Takahashi M, Shoji Y, Takeuchi Y, Matsubara S, Sugimura T, Wakabayashi K. Dose-dependent suppression of hyperlipidemia and intestinal polyp formation in *Min* mice by pioglitazone, a PPAR γ ligand. *Cancer Sci* 2003; 94: 960-4.

[4] Schwarz JM, Linfoot P, Dare D, Aghajanian K. Hepatic de novo lipogenesis in normoinsulinemic and hyperinsulinemic subjects consuming high-fat, low-carbohydrate and low-fat, high-carbohydrate isoenergetic diets. *Am J Clin Nutr* 2003; 77: 43-50.

[5] Whitcomb DC, Lowe ME. Human pancreatic digestive enzymes. *Dig Dis Sci* 2007; 52: 1-17.

[6] Lee B, Zhu J, Wolins NE, Cheng JX, Buhman KK. Differential association of adipophilin and TIP47 proteins with cytoplasmic lipid droplets in mouse enterocytes during dietary fat absorption. *Biochim Biophys Acta* 2009; 1791: 1173-80.

[7] Hussain MM, Pan X. Circadian regulators of intestinal lipid absorption. *J Lipid Res* 2015; 56: 761-70.

[8] Holt PR, Balint JA. Effects of aging on intestinal lipid absorption. *Am J Physiol* 1993; 264: G1-6.

[9] Bouchoux J, Beilstein F, Pauquai T, Guerrero IC, Chateau D, Ly N, Alqub M, Klein C, Chambaz J, Rousset M, Lacorte JM, Morel E, Demignot S. The proteome of cytosolic lipid droplets isolated from differentiated *caco-2/TC7* enterocytes reveals cell-specific characteristics. *Biol Cell* 2011; 103: 499-517.

[10] de Vogel-van den Bosch HM, Büniger M, de Groot PJ, Bosch-Vermeulen H, Hooiveld GJ, Müller M. PPAR α -mediated effects of dietary lipids on intestinal barrier gene expression. *BMC Genomics* 2008; 9: 231.

[11] van den Bosch HM, Büniger M, de Groot PJ, van der Meijde J, Hooiveld GJ, Müller M. Gene expression of transporters and phase I/II metabolic enzymes in murine small intestine during fasting. *BMC Genomics* 2007; 8: 267.

[12] Büniger M, van den Bosch HM, van der Meijde J, Kersten S, Hooiveld GJ, Müller M. Genome-wide analysis of PPAR α activation in murine small intestine. *Physiol Genomics* 2007; 30: 192-204.

[13] Obrowsky S, Chandak PG, Patankar JV, Povoden S, Schlager S, Kershaw EE, Bogner-Strauss JG, Hoefler G, Levak-Frank S, Kratky D. Adipose triglyceride lipase is a TG hydrolase of the small intestine and regulates intestinal PPA-

Intestinal cholesterol absorption in colorectal cancer

- Ralpha signaling. *J Lipid Res* 2013; 54: 425-35.
- [14] Yang R, Han X, Uchiyama T, Watkins SK, Yaguchi A, Delude RL, Fink MP. IL-6 is essential for development of gut barrier dysfunction after hemorrhagic shock and resuscitation in mice. *Am J Physiol Gastrointest Liver Physiol* 2003; 285: G621-G629.
- [15] Davis MR, Arner E, Duffy CR, De Sousa PA, Dahlman I, Arner P, Summers KM. Expression of FBN1 during adipogenesis: relevance to the lipodystrophy phenotype in marfan syndrome and related conditions. *Mol Genet Metab* 2016; 119: 174-85.
- [16] Uchida A, Slipchenko MN, Cheng JX, Buhman KK. Fenofibrate, a peroxisome proliferator-activated receptor alpha agonist, alters triglyceride metabolism in enterocytes of mice. *Biochim Biophys Acta* 2011; 1811: 170-6.
- [17] Nassir F, Wilson B, Han X, Gross RW, Abumrad NA. CD36 is important for fatty acid and cholesterol uptake by the proximal but not distal intestine. *J Biol Chem* 2007; 282: 19493-501.
- [18] Yen CL, Nelson DW, Yen MI. Intestinal triacylglycerol synthesis in fat absorption and systemic energy metabolism. *J Lipid Res* 2015; 56: 489-501.
- [19] Puppa MJ, White JP, Sato S, Cairns M, Baynes JW, Carson JA. Gut barrier dysfunction in the Apc(Min/+) mouse model of colon cancer cachexia. *Biochim Biophys Acta* 2011; 1812: 1601-6.
- [20] Okumura R, Takeda K. Roles of intestinal epithelial cells in the maintenance of gut homeostasis. *Exp Mol Med* 2017; 49: e338.
- [21] Seyer A, Cantiello M, Bertrand-Michel J, Roques V, Nauze M, Bézirard V, Collet X, Touboul D, Brunelle A, Coméra C. Lipidomic and spatio-temporal imaging of fat by mass spectrometry in mice duodenum during lipid digestion. *PLoS One* 2013; 8: e58224.
- [22] Zhou X, Cao L, Jiang C, Xie Y, Cheng X, Krausz KW, Qi Y, Sun L, Shah YM, Gonzalez FJ, Wang G, Hao H. PPARalpha-UGT axis activation represses intestinal FXR-FGF15 feedback signaling and exacerbates experimental colitis. *Nat Commun* 2014; 5: 4573.
- [23] Howles PN, Carter CP, Hui DY. Dietary free and esterified cholesterol absorption in cholesterol esterase (bile salt-stimulated lipase) gene-targeted mice. *J Biol Chem* 1996; 271: 7196-202.
- [24] Febbraio M, Guy E, Coburn C, Knapp FF Jr, Beets AL, Abumrad NA, Silverstein RL. The impact of overexpression and deficiency of fatty acid translocase (FAT)/CD36. *Mol Cell Biochem* 2002; 239: 193-7.
- [25] Yamanashi Y, Takada T, Yoshikado T, Shoda J, Suzuki H. NPC2 regulates biliary cholesterol secretion via stimulation of ABCG5/G8-mediated cholesterol transport. *Gastroenterology* 2011; 140: 1664-1674.
- [26] Colin S, Briand O, Touche V, Wouters K, Baron M, Pattou F, Hanf R, Tailleux A, Chinetti G, Staels B, Lestavel S. Activation of intestinal peroxisome proliferator-activated receptor-alpha increases high-density lipoprotein production. *Eur Heart J* 2013; 34: 2566-74.
- [27] Staels B, Handelsman Y, Fonseca V. Bile acid sequestrants for lipid and glucose control. *Curr Diab Rep* 2010; 10: 70-7.
- [28] Li T, Chiang JY. Regulation of bile acid and cholesterol metabolism by PPARs. *PPAR Res* 2009; 2009: 501739.